



**HAL**  
open science

# Predicting the Type of Nonlinearity of Shallow Spherical Shells: Comparison of Direct Normal Form with Modal Derivatives

Yichang Shen, Nassim Kesmia, Cyril Touzé, Alessandra Vizzaccaro, Loic Salles, Olivier Thomas

## ► To cite this version:

Yichang Shen, Nassim Kesmia, Cyril Touzé, Alessandra Vizzaccaro, Loic Salles, et al.. Predicting the Type of Nonlinearity of Shallow Spherical Shells: Comparison of Direct Normal Form with Modal Derivatives. Second International Nonlinear Dynamics Conference (NODYCON 2021), Feb 2021, Rome, Italy. pp.361-371, 10.1007/978-3-030-81162-4\_32 . hal-04073620

**HAL Id: hal-04073620**

**<https://ensta-paris.hal.science/hal-04073620>**

Submitted on 18 Apr 2023

**HAL** is a multi-disciplinary open access archive for the deposit and dissemination of scientific research documents, whether they are published or not. The documents may come from teaching and research institutions in France or abroad, or from public or private research centers.

L'archive ouverte pluridisciplinaire **HAL**, est destinée au dépôt et à la diffusion de documents scientifiques de niveau recherche, publiés ou non, émanant des établissements d'enseignement et de recherche français ou étrangers, des laboratoires publics ou privés.



Distributed under a Creative Commons Attribution - NonCommercial 4.0 International License

# Predicting the Type of Nonlinearity of Shallow Spherical Shells: Comparison of Direct Normal Form with Modal Derivatives

Yichang Shen<sup>1</sup>, Nassim Kesmia<sup>1</sup>, Cyril Touzé<sup>1</sup>, Alessandra Vizzaccaro<sup>2</sup>, Loïc Salles<sup>2</sup>, and Olivier Thomas<sup>3</sup>

<sup>1</sup> IMSIA, Institut of Mechanical Sciences and Industrial Applications, ENSTA Paris, CNRS, EDF, CEA, Institut Polytechnique de Paris, Palaiseau, France.

<sup>2</sup> Vibration University Technology Centre, Imperial College London, London, UK.

<sup>3</sup> Arts et Métiers Institute of Technology, Lille, France.

**Abstract.** Nonlinear vibrations of free-edge shallow spherical shells with large amplitudes are investigated, with the aim of predicting the type of nonlinearity (hardening/softening behaviour) for each mode of the shell, as a function of the radius  $R$  of curvature of the shell, from the plate case ( $R \rightarrow \infty$ ) to the limit of non-shallow shell. Two different models (based on von Kármán's assumptions or on full numerical finite element approach), and two different methods (normal form and modal derivatives) are contrasted.

**Keywords:** Reduced-order model, hardening/softening behaviour, non-linear normal form, modal derivatives

## 1 Introduction

Reduced-order modelling (ROM) strategies dealing with geometrically nonlinear structures attract attention for a long time and a number of methods have been proposed in the literature. In the recent years, a special emphasis has been put toward applications to finite-element (FE) based models in order to extend the range of application to engineering structures with complex geometries. Also, numerous developments take into account both the *non-intrusive* characteristic of the method, that can be used with a standard (commercial) FE code without the need of entering inside the programs at the elementary level, and also on *simulation-free methods*, that can be used without the need of a priori, offline computations [4, 3].

The aim of this paper is to compare two different methods, namely the quadratic manifold (QM) built from modal derivatives (MD) [2, 5] and the direct normal form approach [7, 11], on a shell example. More particularly, the ability of the two methods in the prediction of the type of nonlinearity (hardening/softening behaviour), is investigated. In nonlinear vibrations, predicting the correct type of nonlinearity is the first characteristics that needs to be correctly given by a ROM since being a fundamental property of the nonlinear oscillations.

The normal form approach, based on the invariant manifold theory, allows such a correct prediction [9]. On the other hand, QM does not rely on invariance property, and it has been shown recently that if a slow/fast assumption is not at hand, incorrect prediction can be formulated [10]. This general result is here illustrated on the specific case of a shallow spherical shell with increasing curvature. For that purpose, the von Kármán model, assuming shallowness, neglecting in-plane and rotary inertia and using an Airy stress function, is used [6].

In a second part, the validity of the von Kármán assumptions are verified by comparing the type of nonlinearity computed from a FE model. For that purpose, the direct normal form approach developed in [11] is used to get a direct access to the hardening/softening behaviour from the FE mesh.

## 2 Modelling

### 2.1 Analytical von Kármán Model for Shallow Spherical Shell

A free-edge spherical shell, made of a homogeneous isotropic material of density  $\rho$ , Poisson's ratio  $\nu$  and Young's modulus  $E$  is considered, with the dimension of thickness  $h$ , radius of curvature  $R$  and outer diameter  $2a$  (see Fig. 1). Large transverse deflections and moderate rotations are considered, so that the model is a generalization of von Kármán's theory for large deflection of plates. The shell is assumed to be thin so that  $h/a \ll 1$  and  $h/R \ll 1$ , and shallow:  $a/R \ll 1$ . Since we are interested in predicting the type of nonlinearity, damping and forcing are not considered. The equations of motion read [6]:

$$D\Delta\Delta w + \frac{1}{R}\Delta F + \rho h\ddot{w} = L(w, F), \quad (1a)$$

$$\Delta\Delta F - \frac{Eh}{R}\Delta w = -\frac{Eh}{2}L(w, w), \quad (1b)$$

where  $w$  is the displacement,  $F$  the the Airy stress function,  $\Delta$  the Laplacian,  $L$  is a quadratic bi-linear operator and  $D = Eh^3/12(1 - \nu^2)$  is the flexural rigidity. The problem is made nondimensional by introducing  $r = a\bar{r}$ ,  $t = a^2\sqrt{\frac{\rho h}{D}}\bar{t}$ ,  $w = h\bar{w}$ , and  $F = Eh^3\bar{F}$ . Thus, substituting the above definitions in equations of motion, Eq. (1), and dropping the overbars in the results, one obtains:

$$\Delta\Delta w + \varepsilon_q\Delta F + \ddot{w} = \varepsilon_c L(w, F), \quad (2a)$$

$$\Delta\Delta F - \sqrt{\kappa}\Delta w = -\frac{1}{2}L(w, w). \quad (2b)$$

where the two nondimensional coefficients are  $\varepsilon_q = 12(1 - \nu^2)\sqrt{\kappa}$ , and  $\varepsilon_c = 12(1 - \nu^2)$ , making also appear the aspect ratio  $\kappa$  of the shell as  $\kappa = \frac{a^4}{R^2h^2}$ .

The complete linear analysis has been tackled in [6]. As an important result, the behaviour of the eigenfrequencies with respect to the aspect ratio  $\kappa$  is shown in Fig. 2. One can observe in particular that purely asymmetric modes ( $k, 0$ ), with  $k$  nodal diameters and no nodal circle, show a very slight dependence

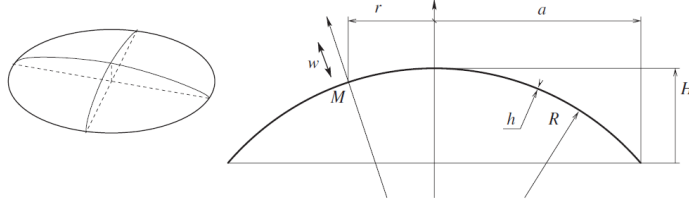


Fig. 1: Geometry of the free-edge shallow spherical shell.

upon  $\kappa$ . On the other hand, axisymmetric modes  $(0, n)$  without nodal diameters, as well as mixed mode  $(k, n)$  with both  $k \neq 0$  and  $n \neq 0$ , show a huge dependence on curvature. These results are important in order to analyze the type of nonlinearity, depending on the mode considered.

In order to predict the type of nonlinearity, Eqs. (2) are projected onto the natural basis of the eigenmodes. After projection, the semi-discretized equations of motion read [6]:

$$\ddot{X}_p + \omega_p^2 X_p + \sum_{i=1}^{+\infty} \sum_{j=1}^{+\infty} g_{ij}^p X_i X_j + \sum_{i=1}^{+\infty} \sum_{j=1}^{+\infty} \sum_{k=1}^{+\infty} h_{ijk}^p X_i X_j X_k = 0, \quad (3)$$

where  $X_p$  refers to the modal amplitude of the  $p$ th transverse mode, and  $\omega_p$  its radian eigenfrequency. The nonlinear coupling coefficients write:

$$g_{ij}^p = -\varepsilon_q \iint_{\varphi_{\perp}} \phi_p L(\phi_i, \psi_j) dS - \frac{\varepsilon_q}{2} \sum_{b=1}^{+\infty} \frac{1}{\xi_b^4} \iint_{\varphi_{\perp}} L(\phi_i, \phi_j) \mathcal{Y}_b dS \iint_{\varphi_{\perp}} \phi_p \Delta \mathcal{Y}_b dS, \quad (4a)$$

$$h_{ijk}^p = \varepsilon_c \sum_{b=1}^{+\infty} \frac{1}{\xi_b^4} \iint_{\varphi_{\perp}} L(\phi_i, \phi_j) \mathcal{Y}_b dS \iint_{\varphi_{\perp}} \phi_i L(\phi_k, \mathcal{Y}_b) dS. \quad (4b)$$

$\phi_i$  refers to transverse eigenmodes while  $\psi_j$  are obtained from the diagonalization of the Airy stress function.  $\xi_n$  and eigenfunction  $\mathcal{Y}_n$  are zeros from the eigenproblem, the interested reader can find their detailed expression in [6].  $\varphi_{\perp}$  is the domain defined by  $(r, \theta) \in [0, 1] \times [0, 2\pi]$ . Eqs. (3) describe the dynamics of the shell and the trend of nonlinearity can be inferred from these equations.

## 2.2 Numerical Finite Element Model

In addition to the von Kármán model developed in the previous section, a FE procedure is also undertaken in order to analyze the type of nonlinearity of shallow spherical shells. For that purpose, the open source software `code_aster` [1] is used, and free-edge shallow shells have been meshed with both 2D shell elements and 3D brick elements. These meshes will be used in order to highlight

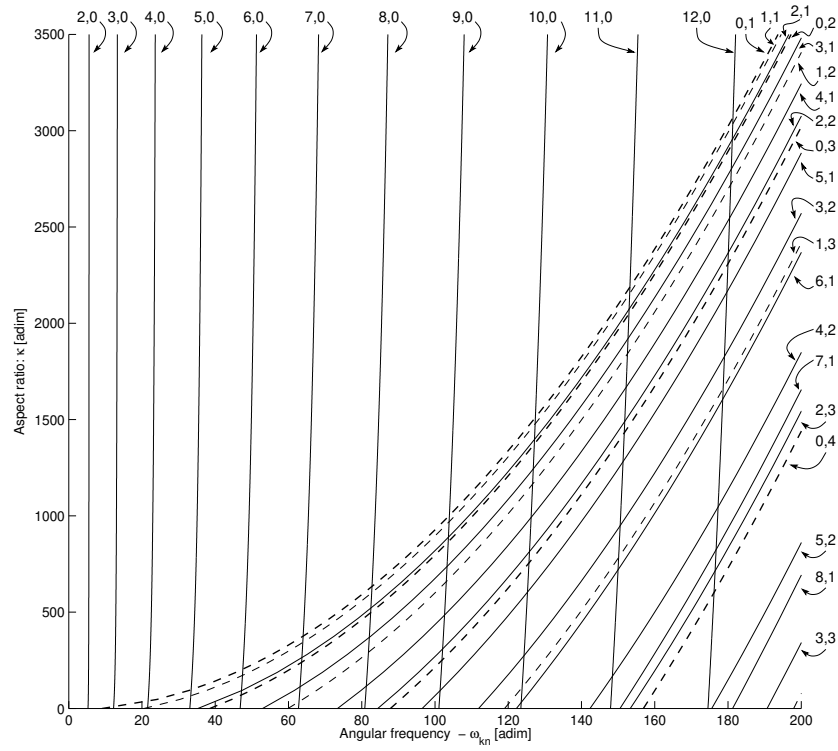


Fig. 2: Dimensionless natural frequencies  $\omega_{kn}$  of the shell as a function of the aspect ratio  $\kappa$  (figure reprinted from [8]).  $\kappa = 0$  corresponds to the flat plate case.

the validity of von Kármán's assumption in order to predict hardening/softening behaviour.

For the geometrically nonlinear structures, the equations of motion stemming from the FE discretization write:

$$\mathbf{M}\ddot{\mathbf{X}} + \mathbf{K}\mathbf{X} + \mathbf{G}(\mathbf{X}, \mathbf{X}) + \mathbf{H}(\mathbf{X}, \mathbf{X}, \mathbf{X}) = \mathbf{0}, \quad (5)$$

where  $\mathbf{X}$  is the vector of generalized displacements at the nodes,  $\mathbf{M}$  is the mass matrix,  $\mathbf{K}$  is the tangent stiffness matrix, and finally,  $\mathbf{G}(\mathbf{X}, \mathbf{X})$  and  $\mathbf{H}(\mathbf{X}, \mathbf{X}, \mathbf{X})$  represents quadratic and cubic nonlinear couplings.

### 3 Analytical Prediction of the Type of Nonlinearity

#### 3.1 Analytical Results from the Three Reduction Methods

We first compare the prediction of the type of nonlinearity using the semi-analytical derivation obtained from von Kármán model. Three different predictions are contrasted. The first one is given by the normal form approach, and

has already been reported in [8]. As known from theoretical results [9], this prediction is correct thanks to the invariance property of nonlinear normal modes (NNMs). Two other solutions are compared to this reference solution, both obtained from the QM approach developed in [2, 5], the first one using full MD, and the second one static modal derivatives (SMD).

In each case, the dynamics is reduced to a single-degree of freedom equation from which one can infer the hardening/softening behaviour. Let  $p$  be the master mode of interest. Following [10], one can show that the reduced dynamics given by the three methods writes:

$$\ddot{R} + \omega_p^2 R_p + C_1 R_p^2 + C_2 \frac{\dot{R}_p^2}{\omega_p^2} + C_3 \frac{\ddot{R}_p R_p}{\omega_p^2} + C_4 R_p^3 + C_5 \frac{\dot{R}_p^2 R_p}{\omega_p^2} + C_6 \frac{\ddot{R}_p R_p^2}{\omega_p^2} = 0, \quad (6)$$

where the expression of  $C_1$  to  $C_6$  are different depending on the method, and are recalled in Tab. 1.

	$C_1$	$C_2$	$C_3$	$C_4$	$C_5$	$C_6$
MD	$g_{pp}^p$	0	0	$h_{ppp}^p - \sum_{s=1, s \neq p}^n \frac{2(g_{pp}^s)^2(\omega_s^2 - 2\omega_p^2)}{(\omega_s^2 - \omega_p^2)^2}$	$\sum_{s=1, s \neq p}^n \frac{4(g_{pp}^s)^2 \omega_p^2}{(\omega_s^2 - \omega_p^2)^2}$	$\sum_{s=1, s \neq p}^n \frac{4(g_{pp}^s)^2 \omega_p^2}{(\omega_s^2 - \omega_p^2)^2}$
SMD	$-2g_{pp}^p$	$-2g_{pp}^p$	$-4g_{pp}^p$	$h_{ppp}^p - \sum_{s=1}^n \frac{2(g_{pp}^s)^2}{\omega_s^2}$	$\sum_{s=1}^n \frac{4(g_{pp}^s)^2 \omega_p^2}{\omega_s^4}$	$\sum_{s=1}^n \frac{4(g_{pp}^s)^2 \omega_p^2}{\omega_s^4}$
NF	0	0	0	$h_{ppp}^p - \sum_{s=1}^n \frac{2(g_{pp}^s)^2(\omega_s^2 - 2\omega_p^2)}{\omega_s^2(\omega_s^2 - 4\omega_p^2)^2}$	$\sum_{s=1}^n \frac{4(g_{pp}^s)^2 \omega_p^2}{\omega_s^2(\omega_s^2 - 4\omega_p^2)^2}$	0

Table 1: Table of coefficients of the reduced dynamics given by the three selected methods: MD for modal derivatives, SMD for static modal derivatives and NF for normal form.

A first-order perturbative development allows definition of the angular frequency of free oscillations  $\omega_{NL}$ , connected to the natural frequency  $\omega_p$ , as  $\omega_{NL} = \omega_p(1 + T_p a^2)$ , where  $a$  is the amplitude of the response of the  $p$ th master coordinate and  $T_p$  the coefficient governing the type of non-linearity.  $T_p > 0$  indicates the hardening behaviour while  $T_p < 0$  implies softening behaviour. The general expression for  $T_p$  with all the  $C_i$  coefficients read as:

$$T_p = -\frac{1}{24\omega_p^4}(10C_1^2 + 10C_1C_2 + 4C_2^2 - 7C_2C_3 + C_3^2 - 11C_1C_3) + \frac{1}{8\omega_p^2}(3C_4 + C_5 - 3C_6). \quad (7)$$

As theoretically shown in [10], the MD and SMD method are awaited to give correct results only if a slow/fast assumption between master and slave coordinates is at hand. This slow/fast assumption has been quantified in [10]. Let  $\rho$  be the ratio between the smallest eigenfrequency of the slave modes and that of the master one labelled  $p$ . If  $\rho > 4$ , the slow/fast (S/F) assumption is fulfilled, while  $\rho < 3$  means that QM method will probably fail. In order to analyze the fulfilment of this S/F, let us introduce  $\rho_p$  for spherical shells as:

$$\rho_p = \min_{n \in E_s} \left( \frac{\omega_n}{\omega_p} \right), \quad (8)$$

where  $E_s$  is the set of all the slave modes, *i.e.* all the modes except the master coordinate  $p$ .

### 3.2 Numerical Results on the Shallow Spherical Shell

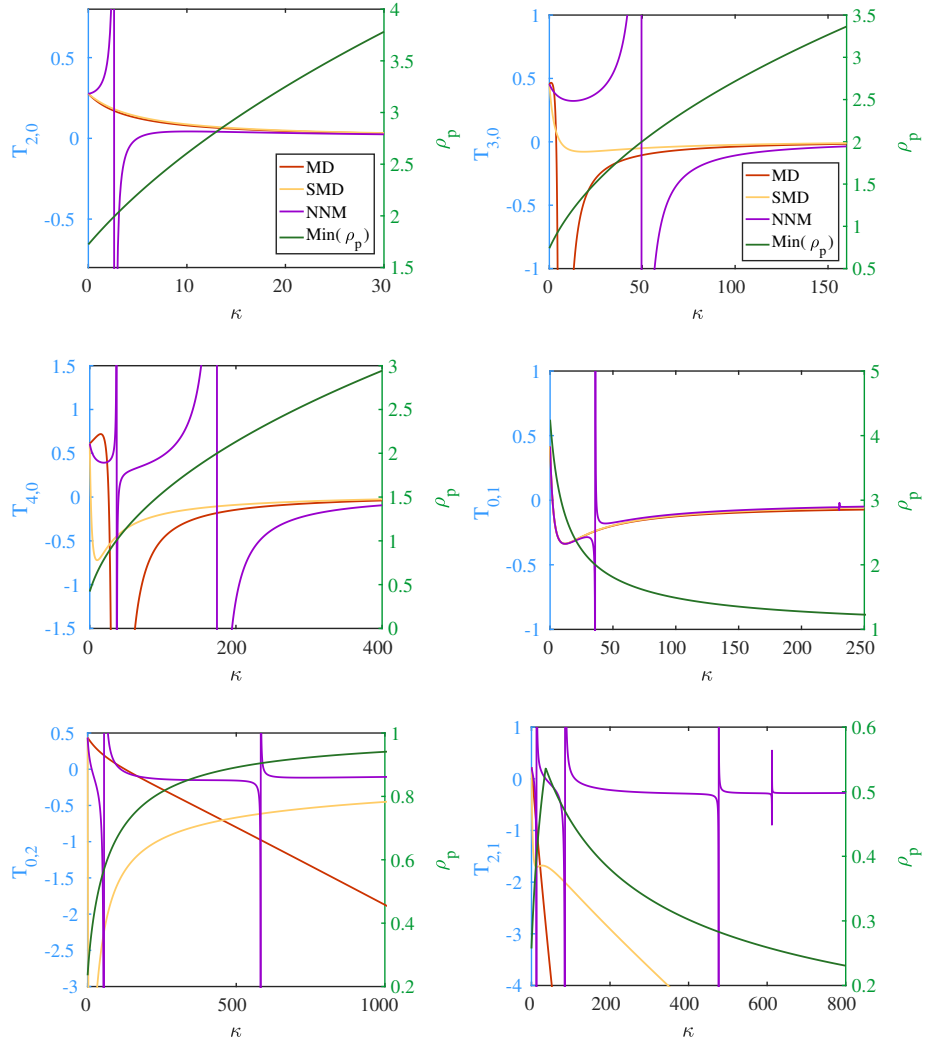


Fig. 3: Type of nonlinearity for 6 modes of the shell: modes (2,0), (3,0), (4,0), (0,1), (0,2), (2,1).

The results are shown for 6 different master modes in Fig. 3. The first three cases are purely asymmetric modes, (2,0), (3,0) and (4,0); then the first two axisymmetric modes are considered, and finally a mixed mode (2,1) is selected. In the figures, the reference solution is given by the normal form approach (NNM) in magenta. The prediction given by QM MD is in red and QM SMD in yellow. The figures have two y-axis allowing to also report the variations of  $\rho_p$  for the mode of interest, as function of  $\kappa$ .

For mode (2,0), one can observe that MD and SMD methods fail to recover the 1:2 resonance leading to a change of behaviour of the type of nonlinearity. On the other hand, when  $\kappa$  is larger than 20, then  $\rho_p$  increases and is close to 4, the S/F assumption is retrieved and the three methods give the same results. Modes (3,0) and (4,0) show another important feature, already noted in [10]: the MD method has a divergence in the case of 1:1 resonance, which has no physical explanation and is interpreted as a failure of the method. For purely asymmetric modes, since they show a very slight dependence on curvature, this means that all the slave modes have strongly increasing eigenfrequencies with  $\kappa$ . Consequently for all these modes the S/F assumption is always finally retrieved, but sometimes at large values of curvature.

Mode (0,1) has the particularity to be very well predicted by using a single linear mode, as shown in [8]. Consequently the three methods behave correctly, even though  $\rho$  is decreasing with  $\kappa$  so that S/F does not hold. As a matter of fact, for all axisymmetric and mixed modes, the behaviour of their eigenfrequencies shown in Fig. 2 underlines that S/F assumption will never been met. Consequently the prediction of the type of nonlinearity given by MD and SMD method completely fails.

## 4 FE Prediction of the Type of Nonlinearity

This section is devoted to compute the type of nonlinearity from FE models. For that purpose, one has first to select a number of specific cases of curvature since continuous increasing of  $\kappa$  is out of reach. Tab. 2 summarizes the selected case, where a constant value of radius  $a=0.15\text{m}$  has been retained. Varying the radius of curvature  $R$  and the thickness  $h$  gives rise to a number of  $\kappa$  values that can be directly compared with the predictions obtained in the previous section.

In the FE model, the material properties of the shell are the following:  $\rho = 4400\text{kg/m}^3$ ,  $E = 1.04e + 11\text{Pa}$ ,  $\nu = 0.3$ . Two types of elements are used in the analysis. In the first case, DKT shell/plate element are used and a mesh composed of 12000 degrees of freedom (dofs), has been built, with three different thicknesses:  $1\text{mm}$ ,  $3\text{mm}$  and  $5\text{mm}$ . In the second case, quadratic 3D element are selected and a mesh composed of approximately 50000 dofs, with the thickness  $3\text{mm}$ , has been created. A careful convergence study has underlined that the eigenfrequencies need to be finely computed in order to obtain a reliable result for the type of nonlinearity.



$a(m)$	0.15									
$R(m)$	3.5	2.5	1.5	0.9	0.8	0.7	0.6	0.5	0.4	0.3
$\kappa(h = 0.001m)$	41.3	81.0	225.0	625	791	1033.16	1406.25	2025	3164.06	5625
$\kappa(h = 0.003m)$	4.59	9	25	69.44	87.89	114.80	156.25	225	351.56	625.00
$\kappa(h = 0.005m)$	1.65	3.24	9	25	31.64	41.32	56.25	81	126.56	225.00

Table 2: Dimensions of the selected shells for the FE analysis with the corresponding  $\kappa$  values.

#### 4.1 Direct Normal Form Approach

In order to predict the hardening/softening behaviour for the FE shell models, the direct normal form (DNF) introduced in [11] is used. The type of nonlinearity can be computed from  $\hat{T}_p$  that reads in this case:

$$\hat{T}_p = \frac{1}{8\hat{\omega}_p^2} [3(\hat{A}_{ppp}^p + \hat{h}_{ppp}^p) + \hat{\omega}_p^2 \hat{B}_{ppp}^p]. \quad (9)$$

In this equation,  $\hat{h}_{ppp}^p$  is the nonlinear cubic coefficient that can be directly computed with a single STEP operation [4]. The other correcting terms  $\hat{A}_{ppp}^p$  and  $\hat{B}_{ppp}^p$  can be directly computed from the FE model thanks to the DNF approach, that allows to go directly from the physical space (nodes of the FE mesh) to the invariant-based span of the phase space, thanks to the nonlinear mapping given by the normal form approach. The complete expressions for leading these computations are explicit in [11], here we simply recall the values of the needed coefficients as given by:

$$\hat{A}_{ppp}^p = 2\phi_p^T \mathbf{G}(\phi_p, \bar{\mathbf{a}}_{pp}), \quad \hat{B}_{ppp}^p = 2\phi_p^T \mathbf{G}(\phi_p, \bar{\mathbf{b}}_{pp}), \quad (10)$$

where the expression of  $\bar{\mathbf{a}}_{pp}, \bar{\mathbf{b}}_{pp}$  can be found in [11].

In order to draw out the comparison with the results obtained in the previous sections (von Kármán model) where a nondimensionalisation was carried out, the relationship between the coefficient computed from FE model  $\hat{T}_p$  and dimensionless  $T_p$  is explicit as:  $T_p = \hat{T}_p h^2 v^2$ , where  $v$  is the mode shape scaling factor, which is chosen to obtain the same maximal amplitude for the analytical and FE mode shapes, i.e.  $\hat{\phi}_p = \phi_p v$ , with  $\phi_p$  normalized by  $\iint_{\varphi_\perp} \phi_p^2 dS = 1$  in analytical von Kármán model.

#### 4.2 Results

Figure 4 compares the analytical result given by von Kármán model and normal form onto the analytical coefficients, to those obtained from the direct computation on the FE model, where again two different types of elements (DKT shell/plate element and 3D elements) have been used. The same mode as in Fig. 3 are used. A perfect matching is obtained between the two methods, underlining

that the von Kármán model, even though relying on numerous assumptions, is sufficient in order to correctly predict the type of nonlinearity of shallow spherical shell. The results also underline the efficiency of the DNF approach for computing accurate ROMs for shell models.

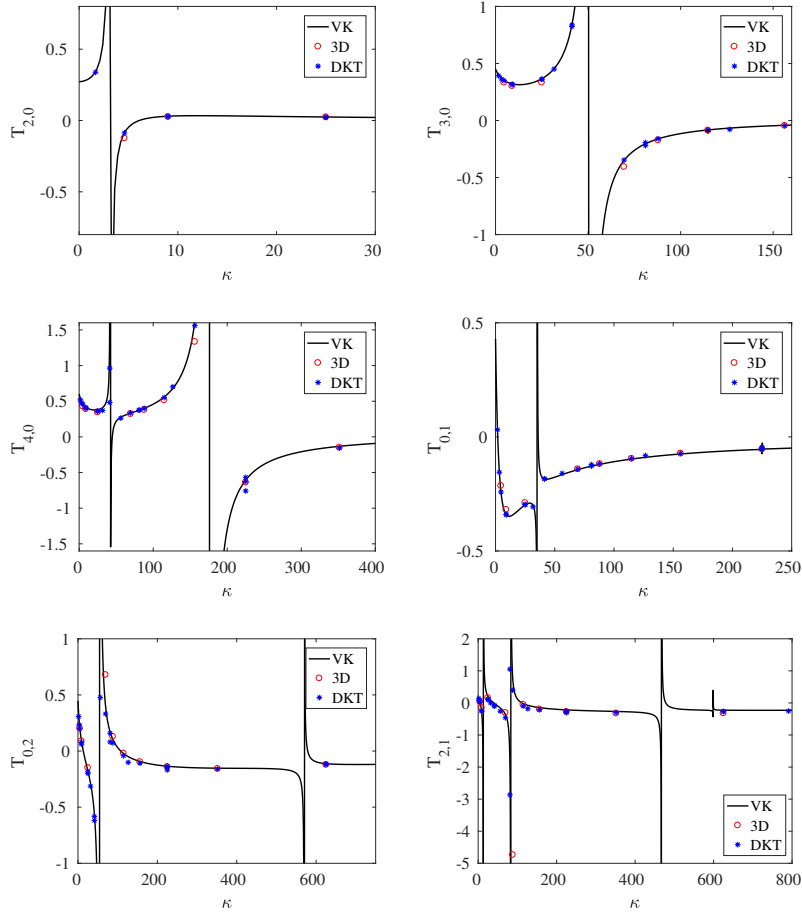


Fig. 4: Type of nonlinearity for 6 modes of the shell: modes (2,0), (3,0), (4,0), (0,1), (0,2), (2,1). Comparison of analytical results from von Kármán model (continuous lines) to numerical predictions obtained by combining FE procedure with DNF.

## 5 Conclusion

The type of non-linearity for free-edge shallow spherical shells has been studied with a special emphasis on comparing different models and methods. Two

methods have been contrasted in their ability to correctly predict the type of nonlinearity: the normal form approach and the QM method based on modal derivatives. In that case, the von Kármán model has been used to illustrate how the two reduction methods can give different predictions. The results underline that modal derivatives approaches need a slow/fast assumption in order to yield a correct prediction. For numerous modes of the shallow spherical shell, the S/F assumption is never met so that both methods (using either MD or SMD) completely fail in predicting correctly the hardening/softening behaviour, whereas the normal form always gives the correct prediction. The second comparison is between the results given by von Kármán model and a finite element procedure. For that purpose, the DNF approach has been used, allowing to directly compute and predict the type of nonlinearity from FE models. Both models have been found to give the same predictions, underlining that the assumptions of the von Kármán model are well fulfilled so that the predictions given are correct.

## References

1. Électricité de France: Finite element *code\_aster*, Analysis of Structures and Thermomechanics for Studies and Research, <https://www.code-aster.org/> (1989-2020).
2. Jain, S., Tiso, P., Rutzmoser, J.B. and Rixen, D.J.: A quadratic manifold for model order reduction of nonlinear structural dynamics. *Comput. Struct.* 188, 80-94 (2017).
3. Mignolet, M.P., Przekop, A., Rizzi, S.A., and Spottswood, S.M.: A review of indirect/non-intrusive reduced order modeling of nonlinear geometric structures. *J. Sound Vib.*, 332, 2437-2460 (2013).
4. Muravyov, A.A. and Rizzi, S.A.: Determination of nonlinear stiffness with application to random vibration of geometrically nonlinear structures. *Comput. Struct.* 81, 1513-1523 (2003).
5. Rutzmoser, J.B., Rixen, D.J., Tiso, P., and Jain, S.: Generalization of quadratic manifolds for reduced order modeling of nonlinear structural dynamics. *Comput. Struct.*, 192, 196-209 (2017).
6. Thomas, O., Touzé, C. and Chaigne, A.: Non-linear vibrations of free-edge thin spherical shells: modal interaction rules and 1:1:2 internal resonance, *Int. J. Solids Struct.* 42(11-12), 3339-3373 (2005).
7. Touzé, C. and Amabili, M.: Non-linear normal modes for damped geometrically non-linear systems: application to reduced-order modeling of harmonically forced structures, *J. Sound Vib.*, 298(4-5), 958-981 (2006).
8. Touzé, C. and Thomas, O.: Non-linear behaviour of free-edge shallow spherical shells: Effect of the geometry. *Int. J. Nonlin. Mech.* 41(5), 678-692 (2006).
9. Touzé, C., Thomas, O. and Chaigne, A. : Hardening/softening behaviour in non-linear oscillations of structural systems using non-linear normal modes , *J. Sound Vib.*, 273(1-2), 77-101 (2004).
10. Vizzaccaro, A., Salles, L. and Touzé, C.: Comparison of nonlinear mappings for reduced-order modelling of vibrating structures: normal form theory and quadratic manifold method with modal derivatives, in press, *Nonlinear Dynamics* (2020).
11. Vizzaccaro, A., Shen, Y., Salles, L., Blahos, J. and Touzé, C. Direct computation of normal form for reduced-order models of finite element nonlinear structures, submitted to *Comput. Method in Appl. Mech. Engng* (2020).